Applied Geochemistry 147 (2022) 105477

Contents lists available at ScienceDirect

Applied Geochemistry

journal homepage: www.elsevier.com/locate/apgeochem

Interlaboratory test for chemical analysis of geothermal fluids: A new approach to determine deep geothermal reservoir fluid composition with uncertainty propagation

Mahendra P. Verma [a,*], Georgina Izquiedo [b], Johannes A.C. Barth [c], Lisette Rayes-Delgado [d], Trupti Chandrasekhar [e], Julienne Eve Algabre [f], Marianne Antonette C. Caballero [g], José Marcus Godoy [h], Mayela Sanchez [i], Lorenzo Brusca [j], Sylvia Malimo [k], Gael Monvoisin [l], Thomas Kretzschmar [m], Ruth Esther Villanueva-Estrada [n], Maria Aurora Armienta [o], Nimal De Silva [p]

[a] *Universidad Politécnica de Nochixtlán "Abraham Castellanos", Carretera a San Mateo Etlatongo Km. 2.5, Asunción Nochixtlán, Oaxaca, C.P., 69600, Mexico*
[b] *Geotermia, Instituto Nacional de Electricidad y Energías Limpias, Reforma 113, Col. Palmira, Cuernavaca, Mor, C.P, 62490, Mexico*
[c] *Friedrich-Alexander-Universität Erlangen-Nürnberg (FAU), Department of Geography and Geosciences, GeoZentrum Nordbayern, Schlossgarten 5, 91054, Erlangen, Germany*
[d] *Campo Geotérmico Los Azufres, Residencia de Estudio, Agua Fría, Michoacán, CP, 61100, Mexico*
[e] *Department of Earth Sciences, IIT Bombay, Powai, Mumbai, 400 076, India*
[f] *Mt Apo Integrated Laboratory Services, Energy Development Corporation - Mt. Apo Geothermal Project, Brgy. Ilomavis, Kidapawan City, 9400, North Cotabato, Philippines*
[g] *Integrated Laboratory Services, Bacman Geothermal Business Unit, Energy Development Corporation, Palayang Bayan, Manito, Albay, Philippines*
[h] *Departamento de Química, PUC-Rio, Vice-decano de Desenvolvimento, Centro Técnico Científico, PUC-Rio, Brazil*
[i] *Empresa Nicaragüense de Electricidad, Dirección de Estudios Geotérmicos, ENEL Central. Pista Juan Pablo II, Intersección Avenida Bolívar. C.P., 13004, Nicaragua*
[j] *Istituto Nazionale di Geofisica e Vulcanologia, Sezione di Palermo, Via Ugo La Malfa, 153, 90146, Palermo, Italy*
[k] *Geothermal Development Company, Polo Centre, Kenyatta Avenue, Nakuru, Kenya*
[l] *Université Paris-Saclay, CNRS, GEOPS, 91405, Orsay, France*
[m] *Centro de Investigación Científica y Educación Superior de Ensenada, Div. Ciencias de la Tierra, Sistema de Laboratorios Especializados, Departamento de geología, Carretera Ensenada-Tijuana #3918, Zona playitas, C.P., 22860, Ensenada, Baja California, Mexico*
[n] *Instituto de Geofísica, Unidad Michoacán, UNAM. Km 8 Antigua carretera a Pátzcuaro 8701, Col. Ex hacienda de San José de la Huerta, Morelia, Mich, C.P., 58190, Mexico*
[o] *Universidad Nacional Autónoma de México, Instituto de Geofísica, Circuito Exterior C.U., CDMX, C.P. 04510, México*
[p] *Room 435A, Advanced Research Complex (ARC), Department of Earth Sciences, University of Ottawa, 25 Templeton Street, Ottawa, Ontario, K1N 6N5, Canada*

A R T I C L E I N F O

Editorial handling by Dr T. H. Darrah

Keywords:
Geothermal water
Inter-laboratory test
Geothermal system
Los Azufres
Geochemical modeling
Uncertainty propagation
NIST Uncertainty machine

A B S T R A C T

A representative fluid sampling of surface geothermal manifestations and its analytical data quality assurance and quality control (QA/QC) are challenging aspects of understanding the geothermal reservoir processes. To achieve these goals, an interlaboratory test for the chemical analyses of ten water samples: one synthetic water, two lake waters (i.e., duplicated), one stream water, and six water samples from two geothermal wells of Los Azufres Geothermal field (LAGF), Michoacan, Mexico, was conducted. The geothermal wells were sampled at four points: (1) total discharge of condensed fluid at the wellhead, (2) separate liquid condensed in the well separator, (3) flushed liquid at the weir box, and (4) separated vapor condensed at the well-separator (data taken from Verma et al., 2022). Sixteen laboratories from ten countries reported their results.

The pH, electrical conductivity, Ca^{2+}, Li^{+}, SO_4^{2-}, B, and Si-total measurements were 8.35 ± 0.04, 12.25 ± 0.53 mS/cm, 25 ± 1 mg/l, 18 ± 1 mg/l, 569 ± 33 mg/l, 320 ± 21 mg/l, and 20.5 ± 0.7 mg/l, which are close to

* Corresponding author.
E-mail addresses: mahendrapverma@upnochixtlan.edu.mx (M.P. Verma), gim@ineel.mx (G. Izquiedo), johannes.barth@fau.de (J.A.C. Barth), lisette.reyes@cfe.gob.mx (L. Rayes-Delgado), trupti@iitb.ac.in (T. Chandrasekhar), algabre.jd@energy.com.ph (J.E. Algabre), carbonel.mr@energy.com.ph (M.A.C. Caballero), jmgodoy@puc-rio.br (J.M. Godoy), msanchez@enel.gob.ni (M. Sanchez), lorenzo.brusca@ingv.it (L. Brusca), SMalimo@gdc.co.ke (S. Malimo), monvoisin.gael@universite-paris-saclay.fr (G. Monvoisin), tkretzsc@cicese.mx (T. Kretzschmar), ruth@geofisica.unam.mx (R.E. Villanueva-Estrada), victoria@geofisica.unam.mx (M.A. Armienta), ndesilva@uottawa.ca (N. De Silva).

https://doi.org/10.1016/j.apgeochem.2022.105477
Received 25 September 2021; Received in revised form 20 June 2022; Accepted 28 September 2022
Available online 7 October 2022

the conventional true values, 8.40, 12.31 mS/cm, 23 mg/l, 19 mg/l, 647 mg/l, 330 mg/l, and 20.0 mg/l, respectively. Analytical errors for major ions, Na^+, Cl^- and CO_2-Total are 17, 21, and 42 percent, respectively; however, the analytical uncertainties are relatively lower, except for CO_2-Total (19%). Similarly, the analytical uncertainty for CO_2-Total measurements of the lake water sample is 18%. Thus, the analytical method of individual laboratories for CO_2-Total measurements needs revision.

The NIST Uncertainty Machine web app was used for the stepwise geothermal reservoir fluid composition calculation with uncertainty propagation from the samples collected at different points of a geothermal well. The wellhead fluid sample does not represent the geothermal reservoir fluid, including the sample collected by connecting a portable separator at the wellhead. The samples collected at points 2 and 3 represent equally well for non-volatile species; however, the sample collected at point 2 is a better representative of geothermal reservoir fluid in analyzing the pH and alkalinity values. It is associated with considering the effect of non-condensable gases (CO_2, H_2S, etc.) liberated at the silencer of the weir box. The geothermal reservoir fluid pH uncertainty, an essential parameter for geochemical modeling, is three to four times the measured fluid pH uncertainty due to the propagation process. Thus, the alkalinity measurement and its calculation procedure of geothermal fluid need revision to understand its correction for the boric, silicic, and other alkalinities.

1. Introduction

Geochemical studies of a geothermal system help advance our understanding of the mechanisms of physical-chemical processes responsible for its formation and evolution (Verma, 2015). The chemical composition of geothermal fluids describes the following reservoir processes: state of water-rock interaction with the variability of cation concentrations (Gianelli and Grassi, 2001), formation of acid-fluid discharge caused by the production-induced pressure at high temperature in the reservoir (Akaku et al., 2000), estimation of cold-water encroachment with chemical monitoring (Wanjie, 2012), fluid flow pattern with silica geothermometry (Verma et al., 1999), production loss due to silica-scaling and corrosion (Andritsos et al., 1976; Gunnlaugsson and Thorhallsson, 2014). Similarly, chemical and isotopic signatures of gaseous species have been observed on the reinjection effect with the variation of gaseous species concentration (Verma et al., 2002b) and non-volatiles species concentration of nearby well-fluids (Arellano et al., 2015), boiling and phase segregation with decreasing concentration of non-volatile components (Scott et al., 2014) and temporal variation of stable isotopes (Nuñez-Hernández et al., 2020), boiling and partial condensation with the distribution of volatile and non-volatile components with well bottom elevation (Nieva et al., 1987). An essential step toward deciphering the reservoir processes is reconstructing geothermal reservoir fluid compositions from the analytical concentrations of surface samples (Scott et al., 2014; Torres-Alvarado et al., 2012).

Ellis (1976) was among the first to recognize the need for analytical data quality control and consistency among geochemical laboratories worldwide to obtain reliable predictions on the reservoir characteristics of a geothermal system reservoir characteristics. He conducted an inter-laboratory comparison among 48 laboratories for seven water samples collected from natural manifestations, including one geothermal water. This exercise resulted in a wide range of results. For example, SiO_2 ranged from 70 to 920 ppm, and HCO_3^- ranged from 1.8 to 50 ppm for the same geothermal water samples. Both species are vital in the geochemical modeling of geothermal systems.

To further understand the scatter in the chemical analyses for individual species in the inter-laboratory comparison results of Ellis' work, Giggenbach et al. (1992) conducted a new interlaboratory comparison for the chemical analyses of three geothermal water samples among 25 laboratories worldwide. They observed that the deficiency in analytical precision and accuracy was one of the most critical limitations in understanding the chemical processes and state of water-rock interaction in natural water bodies. As a result, they emphasized the need for general improvement and standardization of analytical procedures for each chemical species. Since then, the International Atomic Energy Agency (IAEA) has conducted various inter-laboratory comparisons for geothermal waters within the framework of the project, "*Coordinated Research Program on the Application of Isotope and Geochemical Techniques in Geothermal Exploration*" as follows: (i) 22 laboratories from 19 countries (Giggenbach et al., 1992), (ii) 15 laboratories from 7 countries (Gerardo-Abaya et al., 1998), (iii) 26 laboratories from 10 countries (Alvis-Isidro et al., 1999), (iv) 35 laboratories from 16 countries (Alvis-Isidro et al., 2000), (v) 38 laboratories from 23 countries (Alvis-Isidro et al., 2002) and (vi) 31 laboratories from 18 countries (Urbino and Pang, 2004). Verma and co-workers (Verma et al., 2002a, 2012; Verma, 2004) summarized and conducted initial statistical analyses of these geochemical data. The greater uncertainty in the analyses of high SiO_2 concentration samples was associated with direct analyzing or highly diluting the concentrated samples (Verma et al., 2002a, 2012). Recently, Verma et al. (2015) conducted an inter-laboratory comparison for carbonic species concentrations of twelve water samples (four synthetic water, one lake water, four geothermal water, one seawater, and two petroleum water samples) among eight international laboratories worldwide. They proposed a new method for analyzing carbonic species of fluids containing alkalinities of types, carbonic, boric, silicic, etc.

In 2017, the "Mexican Center for Innovation in Geothermal Energy (CeMIE-Geo)" started a further inter-laboratory test project (CeMIE-Geo2017) for analytical quality assurance and quality control of the geochemistry laboratories set up under the CeMIE-Geo consortium. From this study, Verma et al. (2018) presented results for the $\delta^{18}O$ and $\delta^{2}H$ determinations of geothermal waters. They concluded that all the analytical techniques (dual-inlet isotope ratio mass spectrometry (DI-IRMS), continuous flow IRMS (CF-IRMS), and laser absorption spectroscopy (LAS)) provide acceptable values with an overall analytical uncertainty ($\pm 1s$, *where s stands for standard deviation*) of ±0.2‰ and ±2.0‰, respectively, within the 95% confidence level. In addition, stable carbon isotope ratios $\delta^{13}C_{DIC}$ of geothermal fluid were shown to have a wider scattering ($s = \pm 3‰$) (Van Geldern et al., 2013; Verma et al., 2020). Moreover, a first worldwide proficiency test for the CO_2 and H_2S determinations of non-condensable gases of geothermal fluids showed a need to revise both sampling and analytical procedures (Verma et al., 2022).

The present work is a part of the CeMIE-Geo2017 project to investigate the reasons for analytical uncertainties in analyzing geothermal fluids worldwide. It aims to define the correct sampling and analysis procedure for individual parameters of geothermal production wells. In the study presented here, an interlaboratory test was conducted for the chemical analyses of ten water samples to achieve these goals. Each sample set had one synthetic water, two lake water (i.e., duplicated), one stream water, and six water samples of two geothermal wells from Los Azufres, Michoacan, Mexico. We evaluated the analytical uncertainty, accuracy, and reproducibility of these analyses. Moreover, this work implemented a method to calculate deep reservoir fluid compositions with uncertainty propagation from the expected values of each geothermal well sample as the first step in the geochemical modeling of geothermal reservoir processes.

2. Experimental

2.1. Water sampling

In a geothermal system, a mixture of vapor and liquid phases reaches the wellhead from the subsurface geothermal reservoir, separating it into vapor and liquid at the separator. The separator liquid is flushed further into a silencer under atmospheric conditions, and the liquid sample is collected at the weir box. Fig. 1 shows a geothermal production well schematic diagram (Verma et al., 2018). The geothermal fluid may be sampled at four specific points of a production well: (1) total discharge condensed fluid at the wellhead, (2) separated liquid condensed at the well-separator, (3) flushed liquid at the weir box, and (4) separated vapor condensed at the well-separator. Samples were collected by condensing geothermal fluids through a stainless-steel serpentine at all sampling points except for the sampling at the weir box.

Each sample for cation analysis was collected in a 10-L plastic bottle by adding 40 ml of concentrated HNO_3. Anion samples were also collected in 10-L bottles without adding any reactive. The Si-total samples were collected in 5-L plastic bottles. They were diluted in the field by distilled water in the following ratios: geothermal well-fluids, 1:9 ratios, Alchichica lake water, 2:3, and natural geothermal stream water, 1:3). All sample bottles were filled to the brim of each container, leaving no headspace. Each sample was agitated with a magnetic stirrer for 4 h in the INEEL laboratory to ensure homogeneity. The agitation was performed by inserting a magnet into the container and closing the lid to avoid direct contact with the atmospheric environment. Subsequently, the sample was filtered with a Millipore mixed cellulose membrane of 0.45 μm. Table 1 presents information on sample treatments in the field and laboratory for the cation, anion, and Si-total sample sets. The cation and anion samples were filled each into 125 ml high-density polyethylene (HDPE) Nalgene bottles, while the Si-total samples were 65 ml high-density polyethylene (HDPE) Nalgene bottles.

Table 2 presents sample code and numbering for a different analysis type in each sample set. Synthetic sample, INEEL11, was prepared by dissolving analytical grade reagents, Merck of 49.5983 g NaCl, 2.9897 g Na_2CO_3, 4.2672 g NaOH, 8.1270 g KOH, 0.3336 g $Ca(OH)_2$, 0.1832 g $Mg(OH)_2$, 0.5143 g LiOH, 15.1186 g $B(OH)_3$, 12 ml HCl, and 3 ml H_2SO_4 in 8 L of distilled water. For dissolved silica, a commercial standard, SiNIST $(NH_4)_2SiF_6$ in H_2O, was used to prepare another synthetic sample, INEEL12, with a 20 mg/l Si-total concentration. The synthetic sample INEEL12 was included twice for the Si-total analysis only (Table 2). Both synthetic water samples (INEEL11 and INEEL12) were identified as one synthetic sample. In addition, the lake sample,

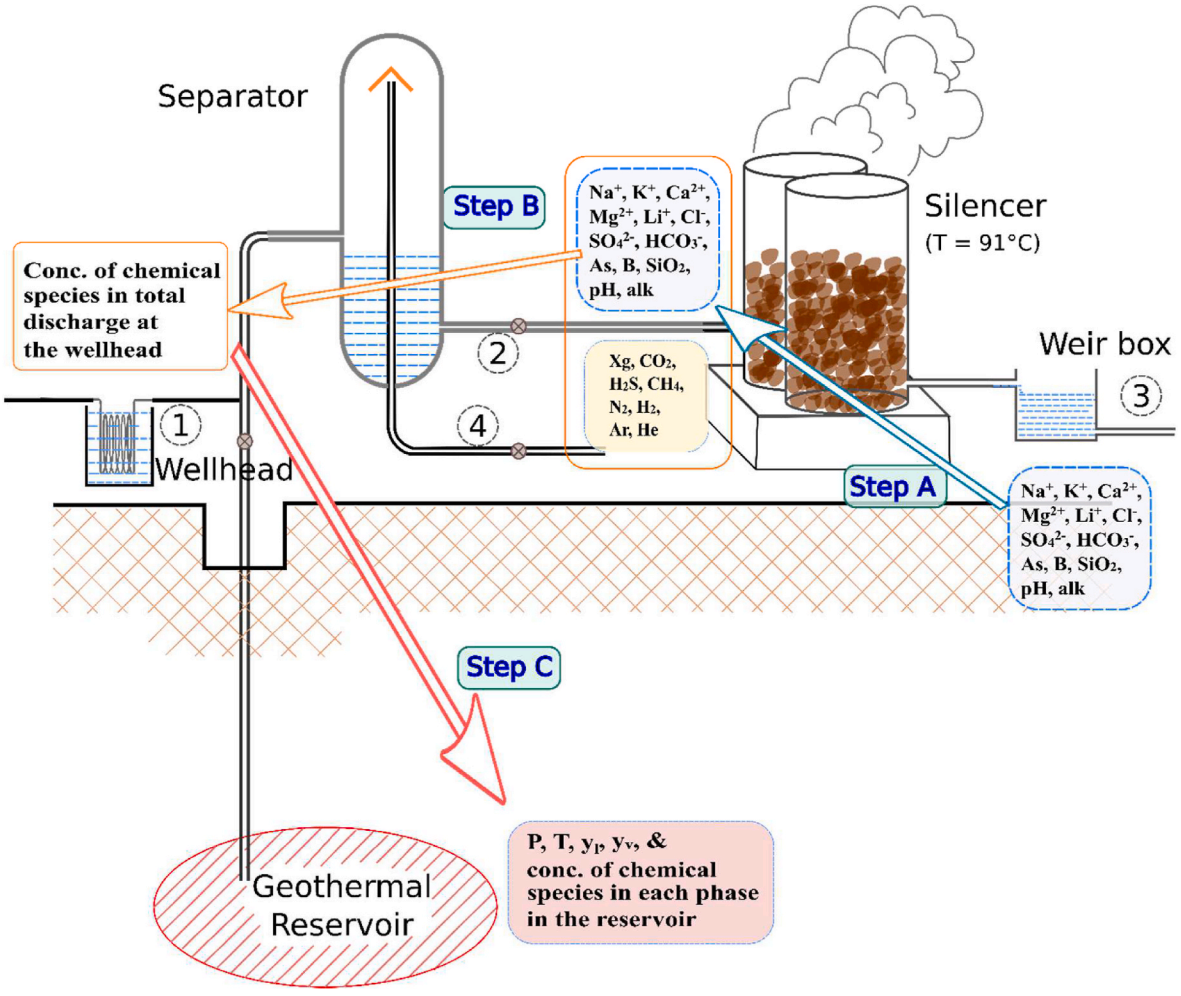

Fig. 1. Location of sampling points at a geothermal well: 1. Total discharge condensed fluid at the wellhead, 2. Separated liquid condensed at the wellhead separator, 3. Flushed liquid at the weir box, and 4. Separated vapor condensed at the wellhead separator. The average elevation at the Los Azufres geothermal wells is 2750 masl (i.e., water boiling point at the surface (Silencer) 91 °C). It also depicts the three steps (A to C) to convert the measured concentrations at sampling locations 3 and 4 to the reservoir fluid chemical composition (Verma, 2013; Verma et al., 2018). Step A calculates the separated liquid concentrations from the measured chemical composition of the water sample collected at the weir box, including the vapor liberated at the silencer. Step B calculates the wellhead total discharge composition from the chemical composition of the separated water and vapor samples at the separator. Step C calculates the geothermal reservoir fluid compositions from the wellhead data calculated in Step B.

Table 1
Sample treatments in the field and laboratory for different types of analysis of geothermal fluid.

Analysis Type	Sample Treatment	Distributed sample amount (ml)	Sample container
Cation:			
Na^+, K^+, Ca^{2+}, Mg^{2+}, Li^+, B-total,	Filtered (0.45 μm) + 4 ml conc. HNO_3 (Suprapur) per 1000 ml sample	125	HDPE plastic/ Nalgene
Si-total	Filtered (0.45 μm) + sample diluted in different proportions with deionized water in the field (see text)	60	HDPE plastic/ Nalgene
Anion:			
pH, HCO_3^- ($+CO_3^{2-}$), Cl^-, SO_4^{2-}	Filtered (0.45 μm)	125	HDPE plastic/ Nalgene

Table 2
Description of water samples distributed under the proficiency test for chemical analysis. The sample sets for cation, anion and Si-total analyses were different, as described in Table 1. Similarly, the sample numbering was different in each set of samples for the different types of analysis. To evaluate the reproducibility of individual laboratories, the Lake water sample INEEL08 was duplicated for the analysis of cations and anions, and the synthetic sample INEEL12 for the Si-total analysis. The synthetic samples, INEEL11 and INEEL12, are considered one synthetic sample in the text and Fig. 3.

Sample Code	Sample numbering in each set			Description
	cation	anion	Si-total	
Az-12D				
INEEL01	1	1	1	Sampled at point 1 in Fig. 1. Condensed total discharge at the Wellhead
INEEL02	2	2	2	Sampled at point 2 in Fig. 1. Condensed liquid at the well separator.
INEEL03	3	3	3	Sampled at point 3 in Fig. 1. Brine at the weir box.
INEEL09				Sampled at point 4 in Fig. 1. Condensed vapor at the well separator for gas and isotope analysis only
Az-23				
INEEL04	4	4	4	Sampled at point 1 in Fig. 1. Condensed total discharge at the Wellhead
INEEL05	5	5	5	Sampled at point 2 in Fig. 1. Condensed liquid at the well separator.
INEEL06	6	6	6	Sampled at point 3 in Fig. 1. Brine at the weir box.
INEEL10				Sampled at point 4 in Fig. 1. Condensed vapor at the well separator
Others				
INEEL07	7	7	7	Water collected at a stream of "Large" lake in the Los Azufres geothermal field (LAGF)
INEEL08	8 9	8 9	8	Water collected from the Alchichica Lake, Puebla, Mexico
INEEL10				Sampled at point 4 in Fig. 1. Condensed vapor at the well separator for gas and isotope ($\delta^{18}O$ and δ^2H) analysis
INEEL11	10	10		Synthetic waters were distributed with
INEEL12			9 10	different ID codes; however, they will be identified as the synthetic sample 10 in the text.

INEEL08, was included twice in the sample sets for cation and anion analyses to evaluate the analytical reproducibility of each laboratory.

Twenty-seven sample sets of each type (cation, anion, and Si-total) were prepared by allocating random sample numbering in each set to maintain individual laboratory secrecy. Twenty-two sets of cation, anion and Si-Total analyses with a unique identification code were distributed as regular test analyses to the laboratories that expressed interest in participating in this exercise from thirteen countries. Four sets were distributed for sample stability test analysis to the four selected laboratories out of the 22. One sample set was kept in the INEEL laboratory to include any other laboratory expressing interest in participating at the last moment and replacing the sample sets mishandled during dispatch, travel, or in the participant laboratory. Sixteen laboratories from ten countries only reported their results. This sample numbering was decoded after receiving the results of all participants.

2.2. Statistics for expected-value estimation

Verma (2013) described the statistical data treatment procedure for assessing the expected values of each sample. First, all evident outliers (misprints or values falling far away from the grouped values) were removed, followed by statistical data treatment. The mean ($\bar{x}$) and standard deviation (s) were calculated for all samples after eliminating all outliers outside two sample standard deviation criteria (i.e., $\bar{x} \pm 2s$). The experiment layout was designed according to the procedure described in the ISO-5752 manual for conducting proficiency tests and evaluating the statistics of the results (ISO, 1994). The sample mean ($\bar{x}$) is an estimate of the population mean (μ), and the sample standard deviation (s) is an estimate of the population standard deviation (σ). Therefore, the symbol 'σ' is reserved for ideal normal distributions comprising an infinite (large) number of measurements (International Association of Geoanalysts,).

The statistical data treatment consisted of:

1. Plotting values of each parameter from all participating laboratories to identify outliers.
2. Determination of means and standard deviations (S.D.) for each parameter (pH, electrical conductivity, Na^+, K^+, Ca^{2+}, Mg^{2+}, Li+, B, Si, CO_2-Total, Cl^-, SO_4^{2-}). Note that carbonic species are generally measured as bicarbonate (and carbonate); however, handling them as the total dissolved carbonic acid is more practical in computer code.
3. Determination of $\bar{x}$ and s for each parameter in the remaining results values to detect outliers with the criteria $\bar{x} \pm 2\ s$; i.e., considering a 95% confidence level.
4. After removing the outliers, $\bar{x}$ and s were computed again, and the values were reported as $\bar{x}$(s) (i.e., $\bar{x} \pm s$, considering the 67% confidence interval).

3. Reservoir fluid composition calculation

Fig. 1 also shows the three steps (A to C) for calculating deep geothermal reservoir fluid characteristics from the measured physical-chemical parameters of separated water and condensed vapor samples obtained from drilled wells. Step A calculates the separated liquid concentrations from the measured chemical composition of the water sample collected at the weir box, including the vapor liberated at the silencer. Step B calculates the wellhead total discharge composition from the chemical composition of the separated water and vapor (data taken from Verma et al., 2022) samples at the separator. Step C calculates the geothermal reservoir fluid compositions from the wellhead data calculated in Step B. The workflow separates total discharge fluid into vapor and liquid at specified pressures (or temperatures) along the liquid-vapor saturation curve (Henley et al., 1984; Verma, 2012).

Fig. 2 presents a block diagram that explains fluid separations into liquid and vapor phases at the separator. The fluid entering into the separator may have three aggregates: 1. vapor only, 2. liquid only, or 3. a mixture of liquid and vapor. In case 1, the vapor will expand in response to the separator pressure. If the pressure change is sudden, part of the vapor condensation may occur due to the adiabatic process when heat loss or gain by the fluid from its surroundings is negligible. Case 1 is unlikely in a geothermal system and will not be considered further.

In cases 2 and 3, the liquid or liquid-vapor phases separate at low

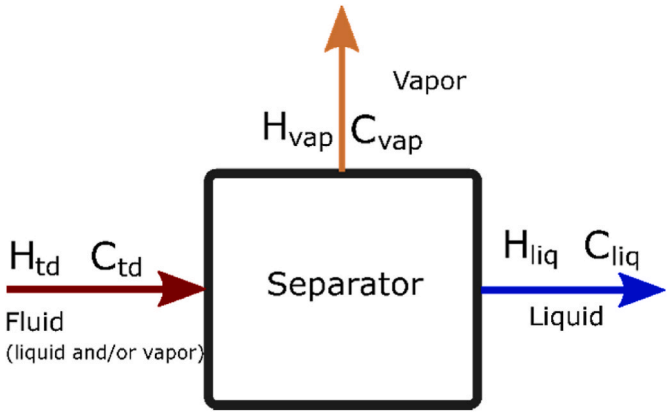

Fig. 2. Block diagram to explain fluid separation into liquid and vapor phases at the separator. H represents enthalpy. C is chemical species concentration. Subscripts (td, vap, and liq) relate to the corresponding parameter for the total discharge, vapor, and liquid, respectively. The calculation procedures will differ if the entering fluid is liquid, vapor, or a mixture of liquid and vapor (see Section 3 for details).

pressure along the water saturation curve. Verma (2012) presented the concentration calculation algorithm. It consists of well-documented equations associated with energy conservation, species distribution, and distribution coefficient for gaseous species (Henley et al., 1984). The equations for these processes are

$$H_{td} = (1-y)\, H_{liq} + y\, H_{vap} \tag{1}$$

$$C_{td} = (1-y)\, C_{liq} + y\, C_{vap} \tag{2}$$

$$D_{coef} = \frac{C_{vap}}{C_{liq}} \tag{3}$$

where H is enthalpy, C is species concentration, y is the fraction of vapor by weight, and subscripts, td, vap, and liq represent the corresponding parameter for the total discharge, vapor, and liquid, respectively. D_{coef} is the gaseous distribution coefficient.

Verma (2012) illustrated the necessity of the fourth equation of alkalinity conservation for these calculations.

$$alk_{td} = (1-y)\, alk_{liq} + y\, alk_{vap} \tag{4}$$

The alkalinity, alk to the acid equivalence point (Stumm and Morgan, 1981), is defined as

$$alk_{td} = [OH^-] - [H^+] + C_{Tcar}(\alpha_{1car} + \alpha_{2car}) + C_{TB}(\alpha_{1B}) + C_{TSi}(\alpha_{1Si}) + C_{TS}(\alpha_{1S}) + C_{TN}(\alpha_{1N}) \tag{5}$$

where the α′s are the ionization fractions and $C_{.T.}$ is the total dissolved concentration of the subscripted constituent, i.e., carbonic acid (car), boric acid (B), silicic acid (Si), hydrogen sulfide (S), and ammonia (N), respectively. In the case of ammonia, the α′s are defined for the corresponding acid (NH_4^+). Thus, the alkalinity expressed here should not change upon dissolution or exsolution of CO_2 (H_2CO_3) and H_2S, but it does change with NH_3 (Stumm and Morgan, 1981). Similarly, the alkalinity will increase or decrease on adding or removing minerals containing the species, bicarbonate (HCO_3^-), carbonate (CO_3^{2-}), silicic ($H_3SiO_4^-$), boric ($B(OH)_4^-$), sulfide (HS^-, S^{2-}), and hydroxide (OH^-). The algorithm does not consider the precipitation of minerals. Consequently, the fluid may be supersaturated in some minerals, such as quartz; however, the time needed for their precipitation was short during the fluid separation into the liquid and vapor phases at the separator and the weir box.

4. Results and discussion

The CEMIE-Geo2017 inter-laboratory test was announced in 2016 via the ISOGEOCHEM List Server (IsoGeochem, 2016) and emailing participants of previous inter-laboratory comparisons (Van Geldern et al., 2013; Verma et al., 2015). The results of the analysis of the regular and stability test sample sets presented by the sixteen participating laboratories were analyzed here for analytical uncertainty, accuracy, and reproducibility.

4.1. Quality assurance and quality control

4.1.1. Synthetic water sample

The synthetic sample, INEEL11, was prepared for cation and anion analyses by dissolving analytical grade reagents. Similarly, INEEL12 for Si-total analysis was a commercial standard Si-NIST $(NH_4)_2SiF_6$. Results in Table 3 for Si-total are from measurements of synthetic sample INEEL12, and the other measurements are from the analysis of synthetic sample INEEL11. The conventional true values of each geochemical parameter are the concentration values based on dissolved minerals' weight (mass) during the sample preparation. Similarly, we measured pH and electrical conductivity before filling samples into individual bottles. Averages of these pH and electrical conductivity values were considered conventional true values.

After analyzing the first sample set, some laboratories analyzed the second sample set for cation, anion, and Si-total after a minimum gap period of one month. The second sample values were noted below the first values for a visual comparison of the analytical data quality of the laboratory (Table 3). The participating laboratories analyzed the second sample set without prior knowledge of concentrations and species distributions with random numbering.

Fig. 3 shows the values of individual laboratories of each parameter of the synthetic sample, INEEL11, and INEEL12 (for Si-Total). Blue circles represent the measured values for the regular samples, while red squares show the values for the stability study samples. The conventional true value (i.e., prepared sample concentration) is plotted with a large thick red dashed line, whereas the average value of all measurements is shown by a solid line (blue). Values marked with red triangles were obvious outliers, while those marked with light blue ellipses remained outliers after the statistical data treatment. The outlier value outside the concentration-axis range is shown in red triangles with its concentration value.

The pH, electrical conductivity, Ca^{2+}, Li^+, SO_4^{2-}, B, and Si-total measurements are 8.35 ± 0.04, 12.25 ± 0.53 mS/cm, 25 ± 1 mg/l, 18 ± 1 mg/l, 569 ± 33 mg/l, 320 ± 21 mg/l, and 20.5 ± 0.7 mg/l, which are close to the conventional true values, 8.40, 12.31 mS/cm, 23 mg/l, 19 mg/l, 647 mg/l, 330 mg/l, and 20.0 mg/l, respectively. The mean value is close to the respective conventional true value and has low variance among the values reported by the individual laboratories. Thus the measurements are precise and accurate.

One must consider the standard deviation and coefficient of variation (C.V.) (BiteSizeBio, 2019). For example, $\bar{x} = 2422$ mg/l, $s = 50$ mg/l, while C.V. is 5.3% for Na^+. Na^+, K^+, Mg^{2+}, and Cl^- have 17, 29, 57, and 21 percent analytical errors, while the C.V. values are 3, 4, 16, and 7, respectively. These observations indicate a need to revise the analytical procedures of their measurements and synthetic sample preparation. Comparing the percentage analytical error (42%) and C.V. (19%) for CO_2-Total determination, it has the most pronounced analytical problem (Table 3); however, carbonic species are critical in geochemical modeling.

Sample, INEEL11, contains 2.9897 g Na_2CO_3, equivalent to 211 mg/l of CO_3^{2-} (i.e., 152 mg/l of total dissolved carbon dioxide (CO_2-Total)). Because the sample pH was 8.40, the carbonate will distribute in the carbonic species, H_2CO_3, HCO_3^-, and CO_3^{2-}, in the proportion of 1.9:210.4:2.4 mg/l, respectively (Table 3). Thus, the dominant species in the sample is bicarbonate. Results of most of the laboratories are in

Table 3
Results of chemical analysis of synthetic water samples, INEEL11 and INEEL12 (for Si-Total only), distributed for the proficiency test as the regular and stability samples. The second value of individual laboratories was noted together to observe the analytical reproducibility.

Lab No.	pH	Elec. Cond	Na^+	K^+	Ca^{2+}	Mg^{2+}	Li^+	B-Total	Cl^-	Carbonic Species				SO_4^{2-}	% charge imbalance	Si-Total
										H_2CO_3	HCO_3^-	CO_3^{2-}	CO_2-Total			
		mS/cm	mg/l	mg/l	mg/l	mg/l	mg/l	mg/l	mg/l	mg/l	mg/l	mg/l	mg/l	mg/l		mg/l
True value																
	8.40	12.31	2902	707	23	9.5	19	330	4396	1.9	210.4	2.4	152	647	1.3	20.0
measured value																
1	8.42	12.55	2363	488	36[b]	4.5	18	306	3600		245.0	12.1	185	601	0.9	20.6
1			2356	481	35	5.2	18	294								20.9
2			2511	497	27	3.6	17	319								19.9
2			2425	503	25	3.7	18	329								20.1
3			2417	489					3245						9.7	
4	8.30	12.67	2421	521	24	2.6	18	354	3552		263.3		190	562	0.8	20.7
4	8.33	12.03							2647		247.0		178	424		20.0
5	8.31	12.71	2451	644	25	6.3	19	281	3539		278.7		201		7.8	20.2
6	8.39	12.45	2408	507	25				3175		322.5		233	594	5.2	20.7
7	8.35		2489	483	21	4.6			3501					547	2.4	19.8
8	8.37	12.10	2467	490	24	4.3	17	323	3600		430.0		310	593	0.5	18.0
9	8.28	12.31	2286	500	25	3.4	25	366	3555	3.0	277.1	3.0	204	697	2.7	22.7
9	8.30	12.35							3440	3.1	303.1	3.5	223	577		
10			2278	489	24	4.4	16	338								22.0
11	8.37	11.13		496	18	4.4	17	251	3519					589	5.1	21.5
11	8.37	10.49							3544					582		
12	8.16	12.30	2487	543	24	4.2	10	330	4234		539.4		389	573	7.1	18.6
12	8.15	12.50							4003		535.8		387	590		
13	8.41	11.10	2513	686					2942		334.3	307.6	467	478	16.7	20.0
14	8.39	12.45	2536	509	24	4.0	17	327	3312		322.5	206.0	384	558	2.4	19.9
15	8.37	12.80							3491							18.1
16			2338	535	26	4.5	20		3440					578	4.7	
Mean	8.35	12.25	2422	502	25	4.12	18	320	3466				216	569		20.5
S.D.[c]	0.04	0.53	80	18	1	0.65	1	21	229				42	33		0.7
C.V.	0.53	4.29	3	4	5	15.85	6	7	7				19	6		3.3
Error (%)	−0.56	−0.52	−17	−29	9	−56.76	−5	−3	−21				42	−12		2.4

[a] Obvious outliers, removed before the statistical analysis of data.
[b] Outliers after the statistical analysis of data.
[c] S.D.– standard deviation, *C.V.* (*Coefficient of Variation*) $= \frac{S.D.}{mean} \times 100$, and *error* (%) $= \frac{(mean - true\ value)}{true\ value} \times 100$

reasonable agreement, even though concentration values are often higher than the sample's true value. However, laboratories 13 and 14 reported the HCO_3^- and CO_3^{2-} concentrations as (334.3 and 307.6 mg/l) and (322.5 and 206.0 mg/l), respectively. When CO_3^{2-} ions are almost absent at pH 8.40, these numbers likely indicate a problem with analysis and reporting carbonic species concentrations.

Verma et al. (2015) concluded that the analytical method to determine carbonic species in geothermal waters could have a conceptual problem. They proposed a revised titration method that measures total carbonic alkalinity and then the total dissolved carbonic species concentration (CO_2-Total). The CO_2-Total concentration distributes in different carbonic species at a given sample pH. Laboratory 9 used this method, and the reported carbonic species concentrations are close to the true values.

4.1.2. Alchichica lake water

Some laboratories analyzed the second sample of the duplicate set at least one month after the analysis of the first sample. The study of the second sample set was to test for potential sample alteration during storage time due to gas liberation and mineral phase precipitation. Additionally, this procedure helped to assess the reproducibility of these laboratories. Table 4 presents a summary of the results of INEEL08. The analytical uncertainty is less than 10% except for Ca^{2+}, Li^+, Cl^-, CO_2-Total, and Si-Total. In the case of Li^+ and Si-Total, the high analytical uncertainty (14 and 13 percent, respectively) is due to their low concentrations. However, a severe problem with the measurement of carbonic species concentrations persisted.

Fig. 4 shows the results of the individual laboratories for each parameter of the lake water samples. The error bar in each data point is calculated for individual laboratory measurements. Blue circles represent the measured values for the regular samples, while red squares show the values for the stability study samples. The solid thick (black) line represents the mean value, and the thin dashed (black) lines show the 95% confidence level (i.e., mean ± 2s). The values marked with dashed red triangles were obvious outliers, while those marked with dashed light blue ellipses were outliers after statistical data treatment. The second set values are close to the first set values for the participating laboratories except for Cl^- of laboratory 4 and SO_4^{2-} of laboratory 9. The error bar in each point is generally within the data point size except for laboratory 11 for Na^+ and B.

Table 5 presents averaged carbonic species concentrations of the lake water sample, INEEL08, measured by individual laboratories. Verma et al. (2015) described three acid-base titration methods to determine carbonic species concentration in natural waters. The hydrologists' and geochemists' methods are based on the location of the two equivalence points, $NaHCO_3EP$ and H_2CO_3EP, while the "initial pH and total alkalinity" method uses the only H_2CO_3EP. The geochemist method also subtracts alkalinities from boric, silicic, ammonium, and hydrogen sulfide compounds.

A sample pH of 9.05 must hold a noticeable carbonate concentration. Laboratories 3, 4, 6, 7, and 8 used the hydrologists' method. They only reported HCO_3^- concentrations obtained by converting the measured carbonic alkalinity to the HCO_3^- species concentration (Verma et al., 2015; Verma, 2005). Laboratories 1, 5, 13, and 14 used the geochemist's

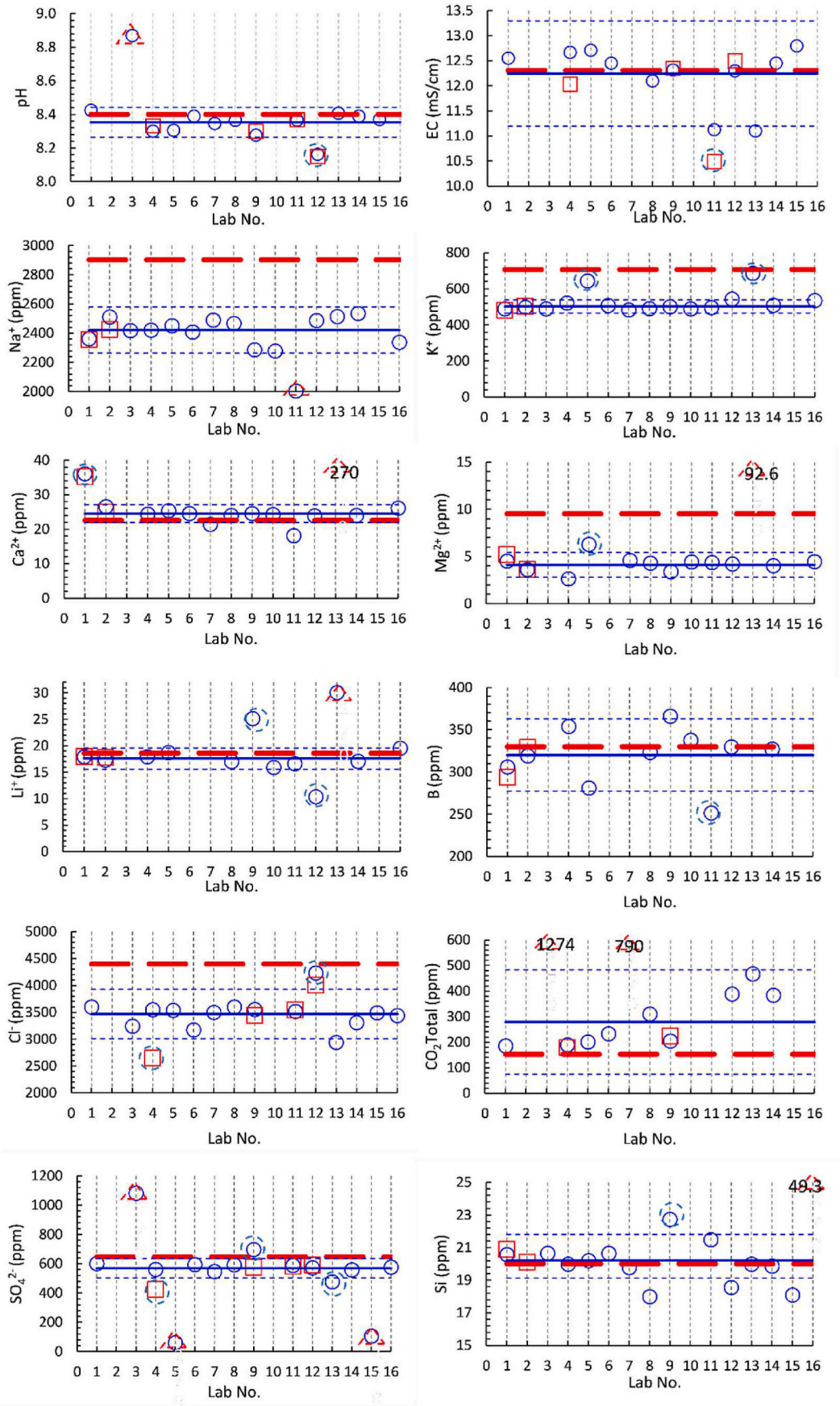

Fig. 3. Comparison of chemical parameter concentration of the synthetic water samples, INEEL11 and INEEL12 (for Si-Total), measured by the participating laboratories. Blue circles represent the measured values for the regular samples, while red squares show the values for the stability study samples. The conventional true value (i.e., prepared sample concentration) is plotted with a dashed line (red), whereas the average value of all measurements is shown by a solid line (blue). The solid thick (blue) line represents the mean values, and the above and below thin dashed (blue) lines show the 95% confidence level (i.e., mean ± 2 S.D.). The values marked with dashed triangles were obvious outliers, while those marked with dashed ellipses were outliers after statistical data treatment. The outlier value outside the concentration-axis range is shown with its concentration value. (For interpretation of the references to colour in this figure legend, the reader is referred to the Web version of this article.)

Table 4
Summary of chemical analysis results of Alchichica lake water samples, INEEL08, distributed as the regular and stability samples for the proficiency test.

Statistics	pH	Elec. Cond	Na^+	K^+	Ca^{2+}	Mg^{2+}	Li^+	B-Total	Cl^-	CO_2Total	SO_4^{2-}	Si-Total
		mS/cm	mg/l	mg/l	mg/l	mg/l	mg/l	mg/l	mg/l	mg/l	mg/l	mg/l
mean	9.05	13.35	2645	245	8.1	470	2.8	43.1	3466	1570	1008	1.25
S.D.	0.09	0.69	94	24	2.2	24	0.4	2.3	407	279	163	0.16
C.V.	0.99	5.13	4	10	27.8	5	14.1	5.4	12	18	16	12.58

method and reported individual concentrations of HCO_3^- and CO_3^{2-}. Laboratory 9 used the third method without considering the contribution of boric and silicic alkalinities. The facts mentioned above may have caused the wide range in the reported values among the individual laboratories and requires another interlaboratory study to investigate the causes of such spreads further.

When using a pH of 9.05 and CO_2Total of 1570 mg/l measured at laboratory temperature of 25 °C (Table 4), one can calculate the carbonic speciation (i.e., H_2CO_3 = 4.21, HCO_3^- = 2064 and CO_3^{2-} = 106 mg/l). These are close to the reported values of laboratory 9. However, at a pH of 9.05, the total dissolved boric concentration will distribute into $B(OH)_3$ and $B(OH)_4^-$. This means if B-total is 320 mg/l (= 29.6 mmol/l); $B(OH)_3$ is 12.9 mmol/l and $B(OH)_4$ is 16.7 mmol/l. In this case, the boric alkalinity (= 16.7 mmol/l) should be subtracted from the total alkalinity to calculate the carbonic alkalinity.

4.1.3. Geothermal waters at LAGF

Table 6 presents the averaged values of geothermal fluids collected from a stream and two production geothermal wells, Az-12D and Az-23, at the Los Azufres Geothermal Field. INEEL07 represents a stream of the "Large" lake in LAGF. Each geothermal well was sampled at the three (1–3) points shown in Fig. 1. The vapor samples (non-condensable gases) data of the wells collected at sampling point 4 were taken from Verma et al. (2022) and are reported in Table 7. The critical observations on the wells data are the following.

1. The analytical uncertainty is higher for geothermal waters than that of synthetic waters. It is associated with matrix effects (Verma et al., 2012); however, it needs an investigation to pinpoint the causes for this behavior of natural geothermal waters.
2. The electrical conductivity is associated with total dissolved solids as well as pH. High electrical conductivity (e.g., INEEL07, the stream water sample) is found at low pH.
3. The participating laboratories did not report the detection limits of measurements for each species. However, the statistical analysis of all the participating laboratories' data shows that the concentration values lower than 2 mg/l (e.g., Mg^{2+} and Li^+) have the same uncertainty order (i.e., the concentration value of a chemical species lower than 2 mg/l has 100% analytical error).

Geochemical calculations (Arnórsson et al., 2006; Henley et al., 1984) are performed considering the liquid sample collection at the weir box and the gas sample (non-condensable gases taken from Verma et al., 2022) at the well-separator. Verma (2012) illustrated stepwise calculations of deep geothermal reservoir fluids and associated problems. These problems occur especially with the concentration of carbonic species at different points along a geothermal well. Therefore, the geothermal fluid samples were collected at four sampling points (Fig. 1) to predict the correct sampling points and procedures for the geochemical characterization of a geothermal system.

Here, we considered the geochemical calculations based on the reported bicarbonate concentration of the individual laboratories as the only carbonic species.

4.2. Geothermal reservoir fluid composition calculation procedure

The code GeoSys.Chem (Verma, 2012) calculates deep geothermal reservoir fluid compositions. However, it does not propagate analytical uncertainty. Therefore, we used the National Institute of Standards and Technology (NIST) Uncertainty Machine, web-based software, to evaluate the measurement uncertainty associated with a scalar or vectorial output quantity using the Gauss and Monte Carlo methods (Lafarge and Possolo, 2020). The approaches are applicable for the output quantity, a given explicit function of a set of scalar input quantities for which estimates, and evaluations of measurement uncertainty are available (Anderson, 1976). This approach was applied to establish the uncertainty propagation in calculating the reservoir fluid composition from the chemical composition of fluid samples collected from geothermal wells.

Table 7 presents the vapor-phase sample's measured chemical composition collected at the geothermal wells' separator, Az-12D and Az-23 (Verma et al., 2022). The concentrations of H_2, NH_3, and N_2 in the non-condensable gas sample are generally low. The study was performed to illustrate the reservoir fluid composition with uncertainty propagation. The species whose concentration is lower than 2 mg/l, like Mg^{2+} are neglected. Thus, the principal elements of the liquid phase are pH, Na^+, K^+, Ca^{2+}, Cl^-, SO_4^{2-}, CO_2-Total, Si-Total, and B-Total. Similarly, the main elements of vapor phase elements are CO_2 and H_2S. The reported values of bicarbonate were converted first to CO_2-Total.

4.2.1. NIST uncertainty machine in geothermal reservoir fluid calculation

In the application of the Gauss and Monte Carlo methods for the uncertainty propagation, Anderson (1976) proposed an algorithm to evaluate the measurement uncertainty associated with an output quantity (y) expressed as an explicit function of input parameters in the following form

$$y = f\,(x_1,\ x_2, \ldots x_n) \tag{6}$$

The variance of y is a function of f and the variances of input parameters $x_1,\ x_2, \ldots x_n$ and is expressed as

$$\sigma_y^2 = \sum_{i=1}^{n}\left(\frac{\partial y}{\partial x_i}\right)\sigma_{x_i}^2 + \sum_{i=1}^{n}\sum_{j=1}^{y}\left(\frac{\partial^2 y}{\partial x_i \partial x_j}\right)\sigma_{x_i x_j} \tag{7}$$

where σ_{x_i} is the uncertainty of the ith variable expressed as unsigned variance, and $\sigma_{x_i x_j}$ is the signed cross-product covariance of all available variables by pairs and defined as

$$\sigma_{x_i}^2 = \frac{\sum_{i=1}^{n}(x_i - \bar{x})^2}{n-1} \quad \sigma_{x_i x_j} = \frac{\sum_{i=1}^{n,n}(x_i - \bar{x})\,(x_j - \bar{x})}{\substack{j=1,\\ i \neq j}\\ n-1} \tag{8}$$

The second double sum vanishes if all the input variables are statistically independent. Even if they depend on each other, their magnitude tends to be small because their signs cancel each other. Thus, the first term is the principal contributor to the variance of the function.

In geochemical modeling, the pH is an implicit function of different types of alkalinities (eq. (5)). Therefore, applying the NIST Machine for uncertainty propagation is not feasible. Kitchin (2013) pointed out the difficulty in the uncertainty propagation to the output variable (y) if it is an implicit function of input parameters ($x_1, x_2, \ldots x_n$). On the other hand, Verma (2022) implemented a method for calculating pH and its uncertainty. The algorithm uses the computer code proposed by Tansey (2021) for converting a uniform random number (0–1) to the Gaussian

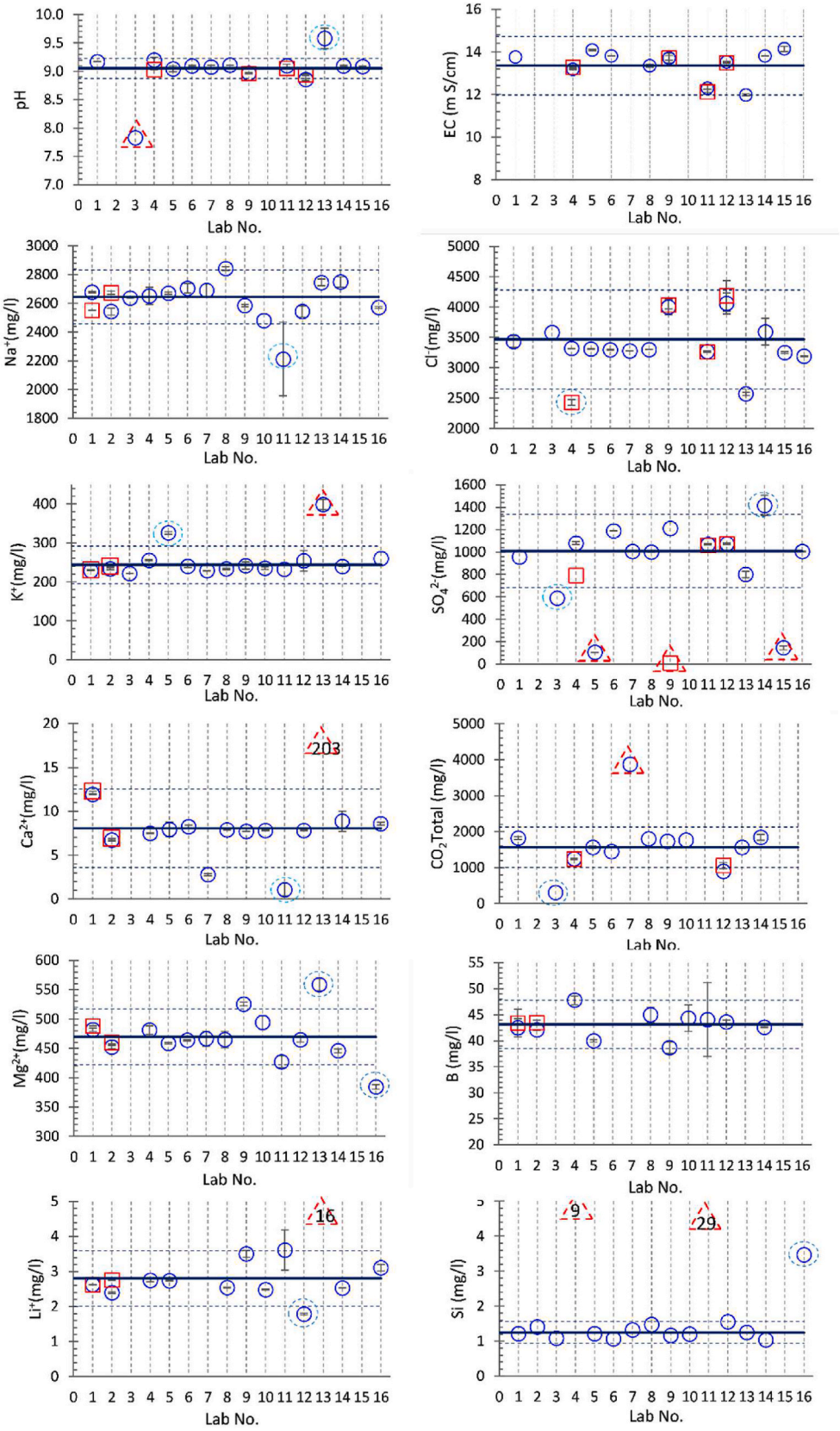

Fig. 4. Comparison of chemical parameter concentration of the lake water samples, INEEL08, measured by the participating laboratories. The error bar in each data point is calculated for individual laboratory measurements. Blue circles represent the measured values for the regular samples, while red squares show the values for the stability study samples. The solid thick (black) line represents the mean values, and the thin dashed (black) lines show the 95% confidence level (i.e., mean ± 2 S. D.). The values marked with dashed red triangles were obvious outliers, while those marked with dashed light blue ellipses were outliers after statistical data treatment. (For interpretation of the references to colour in this figure legend, the reader is referred to the Web version of this article.)

Table 5
Averaged carbonic species concentrations of INEEL08 in mg/l measured by individual laboratories. The value in parenthesis represents the standard deviation (e.g., pH = 9.18(0.06, 0.65) refers to 9.18 ± 0.06 and C.V. = 0.65 with 67% confidence interval and 95% confidence level). At pH = 9.05, the boric alkalinity will be 181 mg/l).

Lab No.	pH	H_2CO_3	HCO_3^-	CO_3^{2-}	CO_2-Total
		mg/l	mg/l	mg/l	mg/l
1	9.18 (0.06, 0.65)		2080(30, 1.4)	409(5, 1.2)	1807 (18, 1.0)
3	7.83(–)		428		309
4	9.12 (0.10, 1.10)		1722(12, 0.7)		1242(8, 0.6)
5	9.00 (0.06, 0.66)		1811(23, 1.3)	370(6, 1.6)	1578 (12, 0.8)
6	9.10 (0.01, 1.1)		2008(70, 3.5)		1449 (50, 3.4)
7	9.08 (0.01, 1.1)		5368(0, 0)		3872(0, 0)
8	9.11 (0.03, 0.33)		2500		1803
9	8.97 (0.00, 0.00)	5.03(0.12, 2.38)	2296(32, 1.4)	123(1, 0.8)	1750 (24, 1.4)
12	8.90 (0.05, 0.56)		1362 (142, 10.4))		983 (103, 10.5)
13	9.58 (0.18, 1.98)		1413(15, 1.1)	748(8, 10.8)	1567(6, 0.4)
14	9.10 (0.01, 1.10)		2008(70, 3.5)	542 (10, 1.8)	1846 (43, 2.3)
From Averaged (Table 4)	9.05 (0.09, 0.99)	3.12 (0.92,29.39)	2030 (361, 18)	106 (38, 27)	1570 (279, 18)

random number for the mean ($\bar{x}$) and standard deviation (s).

4.3. Example calculations considering the data of Az-12D geothermal well

The geochemical data of the geothermal water sample of well, Az-12D, were considered an example to illustrate the deep geothermal reservoir fluid composition calculation procedure. We used the NIST Uncertainty Machine for the uncertainty propagation at each step except for pH because it is impossible to express an explicit equation for pH. First, the charge imbalance (i.e., all the major chemical parameters) was calculated to verify the analysis quality. The chemical analysis datasets with a charge imbalance value of less than 5% in geochemical literature were considered for geochemical calculation data. Our datasets for samples collected at the weir box and the separator satisfy the criteria for both geothermal wells (See Table 8).

4.3.1. Liquid sample collected at the weir box

The water sample analyses were performed at the laboratory temperature (i.e., 25 °C). The concentrations were converted to mmol/l. Then, the total dissolved carbonic acid H_2CO_3* concentration was calculated using the sample pH and HCO_3^- (CO_3^{2-}). Similarly, the speciation of other acid-base species was performed to calculate the total alkalinity (eq. (5)). Table 8 presents the calculated values at each step for both wells, Az-12D and Az-23.

- *Heating liquid sample up to the weir box liquid-vapor separation temperature:* In reconstructing the deep geothermal reservoir fluid composition, the first step is to heat the weir box water sample to the temperature of the silencer (91 °C). (Fig. 1). The well Az-12D had alkalinity of 1.2489 meq/l. It remains a conservative entity when heating the sample from the analysis temperature of 25 °C to the

Table 7
Chemical analysis of vapor samples of geothermal wells, Az-12D and Az-23 (taken from Verma et al., 2022).

Well	Wellhead Pressure (psia)	Separation pressure (psia)	CO_2	H_2S
			mmol of gas/100 mol steam	
Az12D	260	122	254.3 (26.1)	14.2 (0.4)
Az23	277	128	242.6 (29.2)	16.1 (0.6)

Table 6
Averaged values of chemical analysis of geothermal fluids at Los Azufres Geothermal Field. The value in parentheses represents the standard deviation (e.g., 3.34(0.12) refers to 3.34 ± 0.12).

Sampling Point	pH	Elec. Cond. mS/cm	Na^+	K^+	Ca^{2+}	Mg^{2+}	Li^+	B-Total	Si-Total	Cl^-	HCO_3^-	SO_4^{2-}
			mg/l									
Stream at LAGF (INEEL07)												
	3.34 (0.12)	371.8 (49.0)	13.5 (2.5)	15.7 (1.0)	2.03 (0.38)	0.28 (0.17)	0.05 (0.05)	1.6 (0.3)	62.3 (12.4)	14.1 (1.3)	5.4 (7.5)	75.0 (9.8)
Production well at LAGF (Az-12D)												
Wellhead (INEEL01)	6.14 (0.64)	42.6 (3.2)	19.9 (35.5)	3.5 (7.7)	0.4 (0.3)	0.04 (0.09)	0.01 (0.00)	6.3 (1.8)	1.3 (1.8)	1.5 (0.9)	16.9 (10.6)	4.1 (1.5)
Separator (INEEL02)	6.63 (0.14)	12.1 (0.6)	2178.3 (69.7)	586.1 (53.5)	16.9 (3.9)	0.08 (0.12)	32.78 (3.61)	363.4 (31.0)	418.7 (20.0)	4255.5 (503.5)	27.1 (13.1)	26.2 (6.2)
Weir box (INEEL03)	7.18 (0.10)	14.7 (0.7)	2714.7 (63.3)	716.5 (42.2)	21.2 (3.3)	0.08 (0.11)	39.72 (2.37)	450.8 (43.6)	465.0 (60.8)	5109.9 (440.8)	42.2 (20.1)	28.1 (8.9)
Production well at LAGF (Az-23)												
Wellhead (INEEL04)	6.38 (0.32	6.6 (0.3)	1167.9 (35.3)	296.3 (10.9)	9.0 (1.7)	0.08 (0.11)	18.85 (3.01)	169.0 (7.9)	262.2 (14.1)	2132.5 (238.9)	19.7 (4.5)	23.1 (9.0)
Separator (INEEL05)	6.78 (0.19)	8.3 (0.5)	1480.7 (49.2)	378.4 (14.2)	10.8 (2.3)	0.07 (0.11)	24.74 (7.29)	212.4 (23.9)	336.6 (23.9)	2800.4 (292.3)	31.1 (11.0)	37.2 (8.0)
Weir box (INEEL06)	7.54 (0.12)	9.8 (0.5)	1800.3 (54.0)	460.3 (19.1)	12.4 (1.9)	0.05 (0.09)	26.80 (2.13)	260.1 (32.9)	388.1 (32.9)	3349.2 (325.3)	59.6 (33.0)	23.4 (6.6)

Table 8
Measured and calculated chemical compositions of geothermal fluid at different sampling points of geothermal wells, Az-12D and Az-23. The chemical concentrations are expressed in mmol/l. The average elevation at the geothermal wells is 2750 masl (i.e., water boiling point at the surface 91 °C).

parameters	Sample at weir box				Sample at separator		Vapor sample (Verma et al., 2022)		Wellhead		Geothermal Reservoir	
	msd	silencer	dilution	separator	msd	separator	Vapor phase	Liquid phase	msd	calculated	Liquid phase	Vapor phase
	Az-12D (H_R = 2419 kJ/kg, T_R = 250 °C, Psep = 0.879 MPa)											
T (°C)	25	91	91	174.3	25	174.3	174.3	174.3	25		250	250
Vapor frac			0.1565				0.8264			0.8264	0.7774	
pH	7.18 (0.10)	7.01 (0.27)	7.01 (0.31)	7.02 (0.22)	6.63 (0.14)	6.70 (0.51)			6.14 (0.64)		6.76 (0.48)	
Na^+	118.1 (2.6)	118.1 (2.6)	99.6(2.3)	99.6(2.3)	94.6 (3.0)	94.6(3.0)			0.87 (1.54)	16.45 (0.53)	73.88 (2.36)	
K^+	18.3 (1.1)	18.3(1.1)	15.5(0.9)	15.5(0.9)	15.0 ((1.4)	15.0((1.4)			0.09 (0.20)	2.60(0.24)	11.69 (1.07)	
Ca^{2+}	0.53 (0.08)	0.53 (0.08)	0.45 (0.07)	0.45 (0.07)	0.42 (0.10)	0.42 (0.10)			0.01 (0.01)	0.07(0.02)	0.33 (0.08)	
Li^+	5.72 (0.34)	5.72 (0.34)	4.83 (0.29)	4.83 (0.29)	4.72 (0.52)	4.72 (0.52)			0.00 (0.00)	0.82(0.09)	3.68 (0.41)	
B-Total	41.70 (4.03)	41.70 (4.03)	35.17 (3.40)	35.17 (3.40)	33.61 (2.87)	33.61 (2.87)			0.58 (0.17)	5.83(0.50)	26.21 (2.24)	
$B(OH)_3$	41.18 (4.02)	41.21 (4.00)	34.76 (3.37)	34.67 (3.37)	33.50 (2.86)	33.38 (2.86)			0.58 (0.17)		26.11 (2.23)	
$B(OH)_4$	0.52 (0.01)	0.49 (0.29)	0.41 (0.29)	0.50 (0.29)	0.12 (0.06)	0.23 (0.14)			0.00 (0.00)		0.10 (0.13)	
Si-Total	16.56 (2.17)	16.56 (2.17)	13.97 (1.83)	13.97 (1.83)	14.91 (0.71)	14.91 (0.71)			0.05 (0.06)	2.59(0.12)	11.62 (0.56)	
H_4SiO_4	16.52 (2.16)	16.44 (2.15)	13.88 (1.82)	13.76 (1.82)	14.90 (0.71)	14.80 (0.71)					11.54 (0.56)	
$H_3SiO_4^-$	0.04 (0.01)	0.12 (0.07)	0.10 (0.07)	0.20 (0.07)	0.01 (0.01)	0.10 (0.04)					0.08 (0.10)	
CO_2-Total	0.797 (0.32)	0.80 (0.32)	0.67 (0.27)	0.67 (0.27)	0.68 (0.34)	0.68 (0.34)	254.3 (26.1)	0.355 (0.036)	0.74 (082)	131.1 (13.6)	2.52 (0.26)	269.77 (27.70)
H_2CO_3	0.11 (0.05)	0.15 (0.10)	0.13 (0.09)	0.32 (0.09)	0.24 (0.13)	0.45 (0.25)			0.46 (0.57)		2.26 (0.34)	
HCO_3^-	0.69 (0.32)	0.64 (0.27)	0.54 (0.23)	0.35 (0.23)	0.44 (0.22)	0.23 (0.28)			0.28 (0.17)		0.26 (0.30)	
CO_3^{2-}	0.00 (0.00)[a]	0.00 (0.00)	0.00 (0.00)	0.00 (0.00)	0.00 (0.00)	0.00 (0.00)			0.00 (0.00)		0.00 (0.00)	
Cl^-	144.1 (12.4)	144.1 (12.4)	121.6 (10.5)	121.6 (10.5)	120.0 (14.2)	120.0 (14.2)			0.04 (003)	20.83(2/ 47)	93.60 (11.07)	
SO_4^{2-}	0.29 (0.09)	0.29 (0.09)	0.25 (0.08)	0.25 (0.08)	0.39 (0.08)	0.39 (0.08)			0.04 (0.02)	0.05(0.01)	0.21 (0.05)	
H_2S-Total							14.2 (0.4)	0.064 (0.002)		7.33(0.21)	0.37 (0.01)	15.00 (0.42)
H_2S											0.32 (0.06)	
HS^-											0.05 (0.06)	
Alk (meq/l)	1.25 (0.33)	1.25 (0.33)	1.05 (0.38)	1.05 (0.38)	0.57 (.23)	0.57 (0.31)			0.28 (0.17)	0.10(0.04)	0.45 (0.18)	
Charge imbalance (%)	0.96				2.42				41.33			
	Az-23 (H_R = 1784 kJ/kg, T_R = 250 °C, Psep = 0.914 MPa)											
T (°C)	25	91	91	176.0	25	176.0	176.0	176.0	25		250	250
Vapor frac			0.1597				0.5121			0.5121	0.4071	
pH	7.54 (0.12)	7.33 (0.46)	7.33 (0.46)	7.31 (0.34)	6.78 (0.19)	6.80 (0.49)			6.38 (0.32)		6.84 (0.88)	
Na^+	78.3 (2.3)	78.3(2.3)	65.8(2.0)	65.8(2.0)	64.4 (2.1)	64.4(2.1)			50.8 (0.28)	31.3(1.0)	53.0(1.8)	
K^+	11.8 (0.5)	11.8(0.5)	9.9(0.4)	9.9(0.4)	9.7 ((0.4)	9.7((0.4)			7.6(0.3)	4.7(0.2)	8.0(0.3)	
Ca^{2+}	0.31 (0.05)	0.31 (0.05)	0.26 (0.04)	0.26 (0.04)	0.27 (0.06)	0.27 (0.06)			0.22 (0.04)	0.13(0.03)	0.22 (0.05)	
Li^+	3.86 (0.31)	3.86 (0.31)	3.24 (0.26)	3.24 (0.26)	3.6(1.1)	3.6(1.1)			2.72 (0.52)	1.73(0.51)	2.93 (0.86)	
B-Total	24.06 (3.04)	24.06 (3.04)	20.22 (2.56)	20.22 (2.56)	19.65 (2.21)	19.65 (2.21)			15.63 (0.73)	9.543 (1.07)	16.17 (1.82)	
$B(OH)_3$	23.38 (3.00)	23.47 (3.02)	19.72 (2.70	19.67 (2.52)	19.55 (2.86)	19.47 (2.20)			0.58 (0.17)		16.10 (2.22)	
$B(OH)_4$	0.67 (0.16)	0.59 (0.53)	0.49 (0.94)	0.54 (0.42)	0.10 (0.06)	0.17 (0.20)			0.00 (0.00)		0.07 (0.13)	
Si-Total	13.82 (1.17)	13.82 (1.17)	11.61 (0.98)	11.61 (0.98)	11.98 (0.85)	11.98 (0.85)			9.34 (0.50)	5.82(0.41)	9.86 (0.70)	

(*continued on next page*)

Table 8 (*continued*)

parameters	Sample at weir box				Sample at separator		Vapor sample (Verma et al., 2022)		Wellhead		Geothermal Reservoir	
	msd	silencer	dilution	separator	msd	separator	Vapor phase	Liquid phase	msd	calculated	Liquid phase	Vapor phase
H_4SiO_4	13.75 (1.17)	13.62 (1.17)	11.44 (0.99)	11.29 (0.98)	11.97 (0.71)	11.88 (0.85)			0.05 (0.06)		9.80 (0.58)	
$H_3SiO_4^-$	0.06 (0.02)	0.20 (0.19)	0.17 (0.16)	0.32 (0.24)	0.01 (0.01)	0.11 (0.12)			0.00 (0.00)		0.07 (0.15)	
CO_2-Total	1.04 (0.58)	1.04 (0.58)	0.88 (0.46)	0.88 (0.46)	0.70 (0.34)	0.70 (0.34)	242.6 (29.2)	0.35 (0.04)	0.63 (0.82)	124.9 (15.0)	2.82 (0.34)	301.46 (36.40)
H_2CO_3	0.06 (0.04)	0.11 (0.11)	0.09 (0.10)	0.29 (0.10)	0.19 (0.13)	0.43 (0.30)			0.46 (0.57)		2.51 (0.63)	
HCO_3^-	0.98 (0.54)	0.94 (0.53)	0.79 (0.46)	0.59 (0.45)	0.51 (0.22)	0.27 (0.25)			0.28 (0.17)		0.31 (0.63)	
CO_3^{2-}	0.00 (0.00)	0.00 (0.00)	0.00 (0.00)	0.00 (0.00)	0.00 (0.00)	0.00 (0.00)			0.00 (.00)		0.00 (0.00)	
Cl^-	94.5 (9.2)	94.5(9.2)	79.4(7.7)	79.4(7.7)	79.0 (8.2)	79.0(8.2)			60.2 (6.7)	38.4(4.01)	65.0(6.8)	
SO_4^{2-}	0.24 (0.07)	0.24 (0.07)	0.20 (0.06)	0.20 (0.06)	0.39 (0.08)	0.39 (0.08)			0.24 (0.09)	0.19(0.04)	0.32 (0.07)	
H_2S-Total							14.2 (0.4)	0.07 (0.00)			0.43 (0.01)	17.38 (0.49)
H_2S											0.37 (0.11)	
HS^-											0.06 (0.11)	
Alk (meq/l)	1.73 (0.56)	1.73 (0.56)	1.45 (0.48)	1.45 (0.48)	0.62 (.23)	0.57 (0.31)			0.36 (0.17)	0.30(0.15)	0.51 (0.26)	
Charge Imbalance (%)	0.72				1.32				0.72			

[a] Values are lower to report in two decimal places.

silencer (weir box) temperature of 91 °C (Stumm and Morgan, 1981). However, the pH and the distribution of acid-base species will change.

- *Diluting with steam liberated at the weir box silencer:* The liberation of vapor with some non-condensable gases occurs due to the separator liquid flushing at the silencer of the weir box. Verma (2012) pointed out that the liquid-vapor separation process at the silencer was not in equilibrium, and it was difficult to quantify the concentration of liberated gases. Therefore, geochemical calculations were performed considering vapor liberation only at the silencer.
- *Heating liquid sample up to the separator temperature:* The diluted sample at the weir box is heated to the separator temperature (i.e., from 91 to 174.3 °C). The calculation procedure is like that presented in section 3.

4.3.2. Liquid sample collected at the separator

The water sample collected at the separator was also analyzed at the laboratory temperature (25 °C). The data quality assurance and geochemical calculation procedures were the same as in section 3.3.1 for heating from 25 to 174.3 °C (i.e., the separator temperature).

4.3.3. Vapor sample collected at the separator

The concentrations of CO_2 and H_2S in the liquid phase were estimated from the vapor phase using the gaseous species distribution coefficients. The CO_2 concentration was used to verify the measured liquid phase concentration and its distribution equation. However, H_2S concentrations were used for further calculations.

4.3.4. Total discharge sample collected at the wellhead

The liquid phase sample collected at the separator is more representative because it avoids CO_2 liberation at the silencer of the weir box. Therefore, the total discharge fluid compositions at the wellhead were calculated using only the liquid and vapor samples at the separator. Although the acid-base speciation of total discharge for the wellhead sample was calculated, it was not performed in the case of the total discharge sample reconstructed from the liquid and vapor samples at the well separator. The primary goal of this study was only to compare the concentration values.

4.3.5. Geothermal reservoir fluid composition

The average temperature of the Los Azufres geothermal reservoir is 250 °C (Verma et al., 2018). According to the enthalpy balance equation (1), the vapor fraction in the geothermal reservoir is 0.7774 for Az-12D and 0.5121 for Az-23. The reservoir fluid composition was calculated by resolving equations (1)–(5). Similarly, each chemical parameter's uncertainty was obtained using the NIST Uncertainty Machine except for pH.

4.4. Comparative evaluation of geothermal data of Az-12D and Az-23

Table 8 summarizes the geothermal reservoir fluid composition calculation of Az-12D and Az-23. The geochemical calculations of a geothermal reservoir are explained in section 4.3. The weir box and separator samples provide almost the same liquid chemical compositions of non-volatile species at the separator conditions for both wells. Let us observe the concentration values of Na^+, K^+, Ca^{2+}, Li^+, B-Total, Si-Total, Cl^-, and SO_4^{2-} in the column "Separator" under "Sample at weir box" and "Sample at separator" for both wells, Az-12D and Az-23. This similarity in the calculated values assures consistency in the analytical data of all the participating laboratories. However, the concentrations of CO_2-Total are not the same for Az-23. The increase in uncertainty in the geothermal reservoir pH was found because this parameter depends on the concentrations of acid-base species and their uncertainties.

The wellhead sample of the geothermal well Az-12D had a high vapor component, while the sample of Az-23 had a high liquid proportion. Thus, the wellhead fluid sample does not represent the geothermal reservoir fluid. This finding remains true for fluid samples collected by connecting a portable separator at the wellhead.

The fluid pH values at the separator conditions, calculated from the weir box and separator samples, were 7.31 ± 0.34 and 6.80 ± 0.49 for

Az-12D and 7.31 ± 0.34 and 6.80 ± 0.49 for Az-23, respectively (Table 8). The higher pH of the weir box sample likely resulted from the liberation of CO_2 and H_2S at the silencer. Both alkalinity values for separator water obtained from the weir box and separator samples should be the same. However, its values are 1.05 ± 0.38 and 0.57 ± 0.31 for Az-12D and 1.45 ± 0.48 and 0.62 ± 0.23 for Az-23, respectively (Table 8). Presently, it is difficult to explain the differences in these alkalinity values.

5. Conclusions

The first interlaboratory comparison test was to establish the sampling procedure and QA/QC of geochemical analysis of geothermal waters worldwide. The analytical results of the synthetic water sample showed reasonable accuracy and precision in the pH, electrical conductivity, Ca^{2+}, Li^{+}, SO_4^{2-}, B, and Si-total measurements (i.e., 8.35 ± 0.04, 12.25 ± 0.53 mS/cm, 25 ± 1 mg/l, 18 ± 1 mg/l, 569 ± 33 mg/l, 320 ± 21 mg/l, and 20.5 ± 0.7 mg/l, which are close to the conventional true values, 8.40, 12.31 mS/cm, 23 mg/l, 19 mg/l, 647 mg/l, 330 mg/l, and 20.0 mg/l, respectively). However, analytical errors for major ions, Na^{+}, Cl^{-}, and CO_2-Total are 17, 21, and 42 percent, respectively, while the analytical uncertainties are relatively lower, except for CO_2-Total (19%).

The agreement in the two independent analyses of the Lake Alchichica water samples by the participating laboratories reconfirmed the analytical reproducibility of individual laboratories; however, the analytical uncertainty for the CO_2-Total measurements of the lake water sample is 18%. Thus, the analytical method for carbonic species and alkalinity determination of individual laboratories for the CO_2-Total measurements needs revision. The relatively higher analytical uncertainty in the analysis of geothermal waters was probably a matrix effect, which required to be dealt with within the design of future interlaboratory tests.

The outcomes of comparative analysis of geothermal waters sampled at different points of geothermal wells, Az-12D and Az-23 of LAGF: (1) total discharge of condensed fluid at the wellhead, (2) separate liquid condensed in the well separator, (3) flushed liquid at the weir box, and (4) separated vapor condensed at the well-separator can be summarized as follows.

1. The wellhead samples collected at point 1 do not represent the geothermal reservoir fluid. There was a high vapor proportion in the Az-12D wellhead samples, while the Az-23 sample had a high liquid contribution.
2. The same chemical concentration of non-volatile species (Na^{+}, K^{+}, Ca^{2+}, Cl^{-}, SO_4^{2-}, Si-Total, and B-Total) of the liquid phase, reconstructed at the separator temperature and pressure conditions from the samples collected at point 3 and measured at point 2, reconfirmed the good analytical precision and reproducibility of individual laboratories indirectly. For example, both values for Na^{+} are 99.6 ± 2.3 and 94.6 ± 3.0 mg/l, respectively (see Table 8). However, the sample collected at point 2 represents a better geothermal reservoir fluid. It was concluded by analyzing the pH and alkalinity values because the non-condensable gases (CO_2, H_2S, etc.) liberated at the silencer were not considered in the geochemical calculations from the weir box sample.
3. The application of the NIST Machine in the uncertainty propagation of geothermal reservoir fluid geochemical composition indicates the pH as a sensitive parameter in the geochemical modeling of the geothermal system. The geothermal reservoir fluid pH uncertainty, an essential parameter for geochemical modeling, is a consequence of acid-base species and is three to four times more than the measured fluid pH uncertainty due to propagation (see Table 8).

Declaration of competing interest

The authors declare that they have no known competing financial interests or personal relationships that could have appeared to influence the work reported in this paper.

Acknowledgments

The authors appreciate the authorities of INEEL for organizing the proficiency test and the assistance from coordinating members of each participating laboratory to undertake the comparison exercise. Financial supports for sampling (travel grant, material, and courier services expenses) were provided by CeMie-Geo Consortium, financed by SENER-CONACYT (No. 20007032). We also thank the "Comisión Federal de Electricidad" (CFE) and its staff for permitting and facilitating the sampling of two production wells at LAGF. We thank Robert van Galdern for his critical reading of the manuscript. The authors appreciate the reviewer's and editor's constructive suggestions and comments to improve the manuscript's content.

References

Akaku, K., Kasai, K., Nakatsuka, K., 2000. Modeling of formation of acid water discharged from high temperature geothermal reservoir 1–2. In: Proceedings World Geothermal Congress 2000 Kyushu - Tohoku, Japan. May 28 - June 10, 2000: 895 – 900.

Alvis-Isidro, R., Urbino, G.A., Gerardo-Abaya, J., 1999. 1999 Interlaboratory Comparison of Geothermal Water Chemistry under IAEA Regional Project RAS/8/075. Report. IAEA, Vienna.

Alvis-Isidro, R., Urbino, G.A., Pang, Z., 2002. 2001 Interlaboratory Comparison of Geothermal Water Chemistry. Report. IAEA, Vienna.

Alvis-Isidro, R., Urbino, G.A., Pang, Z., 2000. Results of the 2000 IAEA Interlaboratory Comparison of Geothermal Water Chemistry. Report. IAEA, Vienna.

Anderson, G.M., 1976. Error propagation by the Monte Carlo method in geochemical calculations. Geochem. Cosmochim. Acta 40, 1533–1538. https://doi.org/10.1016/0016-7037(76)90092-2.

Andritsos, N., Ungemach, P., Koutsoukos, P., Andritsos, N., Ungemach, P., 1976. Corrosion. Scaling. 3, 181–194.

Arellano, V.M., Barragán, R.M., Ramírez, M., López, S., Aragón, A., Paredes, A., Casimiro, E., Reyes, L., 2015. Reservoir processes related to exploitation in Los Azufres (México) geothermal field indicated by geochemical and production monitoring data. Int. J. Geosci. 1048–1059. https://doi.org/10.4236/ijg.2015.69083, 06.

Arnórsson, S., Bjarnason, J.Ö., Giroud, N., Gunnarsson, I., Stefánsson, A., 2006. Sampling and analysis of geothermal fluids. Geofluids 6, 203–216. https://doi.org/10.1111/j.1468-8123.2006.00147.x.

BiteSizeBio, 2019. https://bitesizebio.com/22776/data-spread-and-how-to-measure-it-the-coefficient-of-variation-cv/. (Accessed July 2021).

Ellis, A.I., 1976. The I . A . G . C . inter-laboratory water analysis comparison programme. Geochem. Cosmochim. Acta 40, 1359–1374. https://doi.org/10.1016/0375-6505(77)90003-7.

Gerardo-Abaya, J., Schueszler, C., Groening, M., 1998. Results of the Interlaboratory Comparison for Water Chemistry in Natural Geothermal Samples under RAS/8/075. Report, Vienna, IAEA.

Gianelli, G., Grassi, S., 2001. Water-rock interaction in the active geothermal system of Pantelleria. Italy. Chem. Geol. 181, 113–130. https://doi.org/10.1016/S0009-2541(01)00276-5.

Giggenbach, W.F., Goguel, R.L., Humphries, W.A., 1992. IAEA interlaboratory comparative geothermal water analysis program. In: Geothermal Investigations with Isotope and Geothermal Techniques in Latin America. IAEA-TECDOC-641, Vienna.

Gunnlaugsson, E., Thorhallsson, S., 2014. Problems in Geothermal Operation – SCALING and CORROSION, Short Course VI on Utilization of Low- and Medium-Enthalpy Geothermal Resources and Financial Aspects of Utilization.

Henley, R.W., Truesdell, A.H., Barton, P.B., 1984. Fluid-mineral Equilibria in Hydrothermal Systems. Society of Economic Geologists, Inc., USA.

IAG. International Association of Geoanalysts. http://www.geoanalyst.org/sigma-is-out/, accessed in July 2021.

ISO, 1994. Accuracy (Trueness and Precision) of Measurement Methods and Results: Part 2: Basic Method for Determination of Repeatability and Reproducibility of a Standard Measurement Method. ISO-5725-2.

IsoGeochem, 2016. First Circular on the Interlab Comparison of Geochemical Analysis of Geothermal Waters, 2017. announced on. https://list.uvm.edu/cgi-bin/wa. (Accessed 30 November 2016).

Kitchin, J., 2013. Uncertainty in Implicit Functions. https://kitchingroup.cheme.cmu.edu/blog/2013/03/08/Uncertainty-in-implicit-functions/. (Accessed July 2021).

Lafarge, T., Possolo, A., 2020. NIST Uncertainty Machine- User's Manual. Version 1.4. NIST.

Nieva, D., Verma, M., Santoyo, E., Barragan, R., Protugal, E., Ortiz, J., Quijano, L., 1987. Chemical and isotopic evidence of steam upflow and partial condensation in Los

Azufres reservoir. In: Proceedings of 12th Workshop on Geothermal Reservoir Engineering. Stanford University, pp. 253–259.

Nuñez-Hernández, S., Pinti, D.L., López-Hernández, A., Shouakar-Stash, O., Martínez-Cinco, M.A., Abuharara, A., Eissa, M.A., Castro, M.C., Ramírez-Montes, M., 2020. Phase segregation, boiling, and reinjection at the Los Azufres Geothermal Field, Mexico, monitored by water stable isotopes, chloride, and enthalpy. J. Volcanol. Geoth. Res. 390, 106751 https://doi.org/10.1016/j.jvolgeores.2019.106751.

Scott, S., Gunnarsson, I., Arnórsson, S., Stefánsson, A., 2014. Gas chemistry, boiling and phase segregation in a geothermal system, Hellisheidi, Iceland. Geochem. Cosmochim. Acta 124, 170–189. https://doi.org/10.1016/j.gca.2013.09.027.

Stumm, W., Morgan, J.J., 1981. Aquatic Chemistry: an Introduction Emphasizing Chemical Equilibria in Natural Waters. Wiley, New York.

Tansey, 2021. Sampling from a Gaussian Distribution in C#. https://gist.github.com/tansey/1444070.

Torres-Alvarado, I.S., Verma, M.P., Opondo, K., Nieva, D., Haklidir, F.T., Santoyo, E., Barragán, R.M., Arellano, V., 2012. Estimates of geothermal reservoir fluid characteristics : GeoSys . Chem and WATCH. Rev. Mex. Ciencias Geol. 29, 713–724.

Urbino, G.A., Pang, Z., 2004. 2003 Interlaboratory Comparison of Geothermal Water Chemistry. Report, PNOC, Philippines.

Van Geldern, R., Verma, M.P., Carvalho, M.C., Grassa, F., Delgado-Huertas, A., Monvoisin, G., Barth, J.A.C., 2013. Stable carbon isotope analysis of dissolved inorganic carbon (DIC) and dissolved organic carbon (DOC) in natural waters - results from a worldwide proficiency test. Rapid Commun. Mass Spectrom. 27, 2099–2107. https://doi.org/10.1002/rcm.6665.

Verma, M.P., 2022. MexInd.GeoSys.Chem: an OOP Computer Code to Estimate Geothermal Reservoir Fluid Characteristics with Uncertainty Propagation. Computer & Geoscience in preparation.

Verma, M.P., 2015. Geothermometry in exploration and exploitation of geothermal system. In: Sharma, U.C., Prasad, R., Sivakumar, S. (Eds.), Energy Science and Technology: Volume 9: Geothermal and Ocean Energy. Studium Press LLC, USA, pp. 96–124.

Verma, M.P., 2013. IAEA inter-laboratory comparisons of geothermal water chemistry: critiques on analytical uncertainty, accuracy, and geothermal reservoir modelling of Los Azufres, Mexico. J. Iber. Geol. 39, 57–72. https://doi.org/10.5209/rev_JIGE.2013.v39.n1.41748.

Verma, M.P., 2012. A GeoSys.Chem : estimate of reservoir fluid characteristics as first step in geochemical modeling of geothermal systems. Comput. Geosci. 49, 29–37. https://doi.org/10.1016/j.cageo.2012.06.001.

Verma, M.P., 2005. Revised analytical methods for the determination of carbonic species in Rain, ground and geothermal waters. Proc. World Geotherm. Congr. 24–29.

Verma, M.P., 2004. A revised analytical method for HCO_3^- and CO_3^{2-} determinations in geothermal waters: an assessment of IAGC and IAEA interlaboratory comparisons. Geostand. Geoanal. Res. 28, 391–409. https://doi.org/10.1111/j.1751-908X.2004.tb00758.x.

Verma, M.P., Izquierdo, G., Urbino, G.A., Gangloff, S., García, R., Aparicio, A., Conte, T., Aurora, M., Sánchez, M., Rizza, J., Gabriel, P., Fajanela, I.D., Renderos, R., Bernadette, C., Acha, A., Prasetio, R., Cruz, I., Reyes, L., Opondo, K., Zendejas, R., Angélica, L., Tapia, R., Lim, P.G., Javino, F., 2012. Geothermics Inter-laboratory comparison of SiO 2 analysis for geothermal water chemistry. Geothermics 44, 33–42. https://doi.org/10.1016/j.geothermics.2012.06.003.

Verma, M.P., Portugal, E., Bernard, R., Reyes-Delgado, L., Chandrasekhar, T., Sanchez, M., Caballero, M.A.C., Malimo, S., 2022. First Worldwide Proficiency Test for CO2 and H2S Analyses of Geothermal Fluids- Assessment on Analytical Procedure. Preparation.

Verma, M.P., Portugal, E., Gangloff, S., Armienta, M.A., Chandrasekharam, D., Sanchez, M., Renderos, R.E., Juanco, M., van Geldern, R., 2015. Determination of the concentration of carbonic species in natural waters: results from a worldwide proficiency test. Geostand. Geoanal. Res. 39 https://doi.org/10.1111/j.1751-908X.2014.00306.x.

Verma, M.P., Santoyo, S., Aragon, A., Fernandez, M.E., Tovar, R., Casimiro, E., Sandoval, F., Johnson, C., Gerardo-Abaya, J., 1999. Geochemical and isotopic monitoring of rainwater in the Los Azufres and Los Humeros zones, relation to geothermal fluids. Geotermia 15.

Verma, M.P., Tello, E., Sandoval, F., Tovar, R., Martinez, J.L., 2002a. An interlaboratory calibration of silica for geothermal water chemistry. Geothermics 31, 677–686. https://doi.org/10.1016/S0375-6505(02)00030-5.

Verma, M.P., Tello, E., Suárez, M.C., González, E., 2002b. Variation of gaseous species concentration in the Los Azufres geothermal wells as a tool to study the reinjection effect. Geofisc. Int. 41.

Verma, M.P., van Geldern, R., Barth, J.A.C., Monvoisin, G., Rogers, K., Grassa, F., Carrizo, D., Huertas, A.D., Kretzschmar, T., Villanueva-Estrada, R.E., Godoy, J.M., Mostapa, R., Cortés, H.A.D., 2018. Inter-laboratory test for oxygen and hydrogen stable isotope analyses of geothermal fluids: assessment of reservoir fluid compositions. Rapid Commun. Mass Spectrom. 32, 1799–1810. https://doi.org/10.1002/rcm.8233.

Verma, M.P., van Geldern, R., Carvalho, M.C., Delgado-Huertas, A., Monvoisin, G., Carrizo, 2020. Interlaboratory test for stable carbon isotope analysis of dissolved inorganic carbon in geothermal fluids. Rapid Commun. Mass Spectrom. 34, 1–12. https://doi.org/10.1002/rcm.8685.

Wanjie, C., 2012. Geochemical monitoring of reservoir response to production. In: Short Course on Exploration for Geothermal Resources, Organized by UNU-GTP, GDC and KenGen, at Lake Bogoria and Lake Naivasha, pp. 1–12. Kenya, 2012.